

Electric dipole moment of the neutron from a flavor changing Higgs-boson

Jan O. Eeg*

*Department of Physics, University of Oslo,
P.O.Box 1048 Blindern, N-0316 Oslo, Norway*

We consider neutron electric dipole moment contributions induced by flavor changing Higgs boson couplings to quarks. Previously one loop diagrams with such couplings were considered in order to constrain quadratic expressions of Higgs flavor changing coupling to quarks. In the present paper the analysis is extended to the two loop level where the large SM Yukawa coupling for Higgs to top, as well as the large SM Higgs coupling to the W-boson, compensates for the loop suppression factor. In the two loop case it is possible to generate diagrams with a flavor changing Higgs coupling to first order *only*. Some contributions contain divergent loops and these divergent contributions do not cancel among themselves. This means that a theory with just the simple term with a flavor changing coupling considered here is not renormalizable. The divergent loops are parametrized in terms of a cut-off Λ . The current experimental bound on the neutron electric dipole moment impose constraints on Higgs flavor changing couplings. We obtain a bound for a certain combination of CKM entries and the flavor changing Higgs coupling. For cut-offs of order one to three TeV, the bound is of the same order of magnitude as the one reported by other authors for the absolute value obtained previously from $B - \bar{B}$ -mixing.

Keywords: CP-violation, Electric dipole moment, Flavor changing Higgs.

PACS: 12.15. Lk. , 12.60. Fr.

*Electronic address: j.o.eeg@fys.uio.no

I. INTRODUCTION

An electric dipole moment (EDM) for elementary particles is a CP-violating quantity and it gives important information on the matter anti-matter asymmetry in the universe. Standard Model (SM) EDMs of elementary fermions are induced through the Cabibbi-Kobayashi-Maskawa (CKM) CP-violating phase. EDMs are studied also within many models Beyond the SM (BSM). For reviews on SM and BSM EDMs, see[1–4]. Experimentally only bounds on electron, muon, proton and neutron EDMs are determined [5]. Explicitly, for the EDM of the neutron (nEDM = d_n) discussed in this paper, the present experimental bound is [6]

$$d_n^{exp}/e \leq 2.9 \times 10^{-26} \text{ cm} . \quad (1)$$

Within the SM, the nEDM is calculated to be several orders of magnitudes below the experimental bound. Calculations of the nEDM will in general put bounds on hypothetical models BSM, and any measured nEDM significantly bigger than the SM estimate (10^{-32} to $10^{-31} e \text{ cm}$) would signal New Physics.

The SM contributions to the nEDM are well known and thoroughly explained in [1]. At a low energy scale one can construct an effective Lagrangian

$$\mathcal{L}_{\text{eff}} = \mathcal{L}_4 + \mathcal{L}_5 + \mathcal{L}_6 + \dots , \quad (2)$$

with all possible CP-odd operators of appropriate dimension. The QCD-odd term gives the dimension 4 operator [1, 7]. The dimension 5 operator contains electric dipole moment operators as well as color electric operators of quarks. The CP-odd three-gluon Weinberg operator and four-fermion interaction are then in the class of dimension six operators [1–3], which are not subject of our study. The electric dipole moment of single fermion in (2) has the form

$$\mathcal{L}_{5,\text{em}} = \frac{i}{2} d_f \bar{\psi}_f \sigma_{\mu\nu} F^{\mu\nu} \gamma_5 \psi_f , \quad (3)$$

where d_f is the electric dipole moment of the fermion, ψ_f is the fermion (quark) field, $F^{\mu\nu}$ is the electromagnetic field tensor, and $\sigma_{\mu\nu} = i[\gamma_\mu, \gamma_\nu]/2$ the dipole operator in Dirac space. The electric dipole operator in (3) for quarks appears within the SM from three loop diagrams with double Glashow-Iliopoulos-Maiani (GIM)- cancellations and a gluon exchange of order $\alpha_s G_F^2$, and is proportional to quark masses and an imaginary CKM factor. These contributions were found to be very small, of order $10^{-34} e \text{ cm}$ [8, 9].

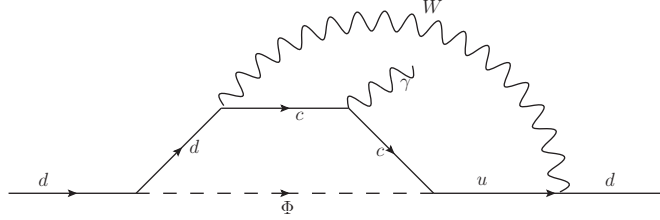


FIG. 1: Two loop diagram for an EDM of a d -quark generated by a FC scalar $c \rightarrow u$ coupling.

Contributions to the nEDM due to interplay of quarks in the neutron, in terms of baryon poles models, were studied in [10–12]. Later chiral perturbation theory was applied, as explained in [1, 7, 13, 14]. Within such mechanisms the d_n was estimated to be of order 10^{-33} to $10^{-31}e$ cm. But these results have large hadronic uncertainties and are therefore rather model dependent.

As mentioned in [15–17], higher dimension operators can be responsible for nEDM. One of these contributions, usually called “diquark mechanism” induces a CP-violating two loop diagram for the quark process $ud \rightarrow du\gamma$. This mechanism, although suppressed by a small hadronic matrix element, still gave 10^{-33} to $10^{-32}e$ cm. It has also been pointed out in [18] that there is a loop-less nEDM within the SM due to an 8-dimensional operator.

The nEDM due to EDMs of light u - and d -, and even s -quarks are given by the formula

$$d_n = \gamma_u d_u + \gamma_d d_d + \gamma_s d_s , \quad (4)$$

similar to a corresponding magnetic moment formula. In the strict valence approximation,

$$\gamma_u = -\frac{1}{3} , \quad \gamma_d = \frac{4}{3} , \quad \gamma_s = 0 , \quad (5)$$

while recent lattice calculations [19, 20] give

$$\gamma_u = -0.22 \pm 0.03 , \quad \gamma_d = 0.74 \pm 0.07 , \quad \gamma_s = 0.008 \pm 0.010 . \quad (6)$$

Note that there is a contribution to the nEDM from the EDM of the s -quark, with a small coefficient.

Many models BSM suggest possible contributions of new particles or new interactions to nEDM [1–4, 7, 21–29]. In the case of New Physics presence, flavor physics might give a number of useful CP-violating observables. These occur in $K^0 - \bar{K}^0$, $D^0 - \bar{D}^0$, $B_{d;s} - \bar{B}_{d;s}$

oscillations as well as a consequence of direct CP-violation which is testable through CP-violating asymmetries in mesonic decays [22, 23, 30]. In such processes one of possible mechanisms generates new contributions to the electric dipole moments of quarks due to New Physics particles coupling to SM quarks (see e.g. [31]). This mechanism is illustrated by the diagram in Fig. 1. In general, this mechanism appears for scalar generated flavour changing couplings for fermions with the same electric charge.

The properties and couplings of the Higgs boson (H) are still not completely known. For instance, the SM Higgs might mix with higher mass scalar(s) in BSM. Some authors [32–36] have suggested that the physical Higgs boson might have flavor changing (FC) couplings to fermions which might also be CP-violating. In these papers bounds on quadratic expressions of such couplings are obtained from various processes, say, like $K - \bar{K}$, $D - \bar{D}$, and $B - \bar{B}$ - mixings, and also from leptonic flavor changing decays like $\mu \rightarrow e \gamma$ and $\tau \rightarrow \mu \gamma$. In the latter case two loop diagrams of Barr-Zee type [37] were also considered [32–34, 38]. (See also [39]). It should be noted that the mechanism shown in Fig. 1 will also give a contribution from couplings proposed in [32–36], when the color scalar is replaced by an ordinary Higgs-boson. Some of such diagrams give contributions suppressed by the small mass ratio m_d/M_W for the ordinary SM Higgs coupling to fermions. (M_W denotes the mass of the W -boson and m_q is the mass of the quark q). However, if the Higgs is coupled to a top (t) quark one might obtain relevant non-suppressed contributions. Motivated by the result of our previous work [31], we consider such diagrams in the next section. There are additional reasons to extend the analysis in [33, 34] for nEDM to two loop level. Namely, it will be demonstrated in the next sections that one might obtain amplitudes with the unknown couplings to first order only. Also, it is known that some two loop diagrams might give bigger amplitudes than one loop diagrams because of helicity flip(s) in the latter [33, 34, 38, 40]. Our two loop amplitudes will be proportional to a large ttH coupling or a large WWH coupling within the SM, in contrast to the small SM Higgs couplings to light fermions. This might compensate for the two loop suppression of our diagrams. In the next section (II) we will present the framework for the FC Higgs couplings. In the following sections (III and IV) we will present our two loop calculations. In section V we discuss the results, and in section VI a conclusion is given. Some technical details are given in the Appendix.

II. FLAVOR CHANGING PHYSICAL HIGGS?

Within the framework in [32–36] the effective interaction Lagrangian for the FC transition $f_1 \rightarrow f_2$ due to Higgs exchange can in general be written

$$\mathcal{L}_{\text{eff}} = Y_R(f_1 \rightarrow f_2) \cdot \overline{(f_2)_L} H (f_1)_R + Y_L(f_1 \rightarrow f_2) \cdot \overline{(f_2)_R} H (f_1)_L + h.c. , \quad (7)$$

where $f_{1,2}$ are fermion fields, H the Higgs field and $Y_{L,R}(f_1 \rightarrow f_2)$ are coupling constants. Thus the hypothetical FC coupling for physical Higgs exchange has the form (in quark and lepton cases):

$$G_H(f_1 \rightarrow f_2) = Y_L(f_1 \rightarrow f_2) \cdot P_L + Y_R(f_1 \rightarrow f_2) \cdot P_R , \quad (8)$$

where $P_L = (1 - \gamma_5)/2$ and $P_R = (1 + \gamma_5)/2$ are the projectors in Dirac space. The Y 's are in general thought to be complex numbers. Then, from the hermitean conjugation part we obtain for the opposite $f_2 \rightarrow f_1$ transition

$$Y_L(f_2 \rightarrow f_1) = Y_R(f_1 \rightarrow f_2)^* \text{ and } Y_R(f_2 \rightarrow f_1) = Y_L(f_1 \rightarrow f_2)^* . \quad (9)$$

Explicitly, for our quark transitions to be used for EDM of a d -quark we need

$$\mathcal{L}_{\text{eff}}^d = Y_R(d \rightarrow q) \bar{q}_L H d_R + Y_L(d \rightarrow q) \bar{q}_R H d_L + h.c. , \quad (10)$$

where $q = s, b$, and similarly for EDMs of the u -quark we need

$$\mathcal{L}_{\text{eff}}^u = Y_R(u \rightarrow q) \bar{q}_L H u_R + Y_L(u \rightarrow q) \bar{q}_R H u_L + h.c. , \quad (11)$$

for $q = c, t$.

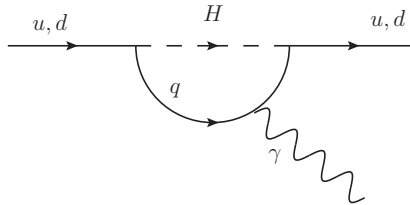


FIG. 2: One loop diagrams for EDMs of u - and d -quarks with FC Higgs couplings.

Using the assumptions based on (7), one obtains one loop diagrams for EDMs of u - and d -quarks [33, 34]. The one loop diagram in Fig. 2 puts bounds on quadratic expressions of the Y 's for definite choices of flavor. Note that this diagram is finite. However, as will be discussed later, the theory based on (7) contains divergent terms which do not cancel among themselves or cannot be hidden in some coupling, meaning that the theory is non-renormalizable. In [33] $\Lambda = 1$ TeV is used as a cut off for a theory based on (7). It should also be pointed out that standing alone the interaction (7) is not $SU(2)_L \times U(1)_Y$ -invariant, and thereby incomplete, such that the non-renormalizability is expected.

III. DIAGRAMS WITH ONE FC COUPLING -AND A $t\bar{t}H$ -COUPLING

In Fig. 3 we show two loop diagrams (a soft photon is assumed to be added) for the EDM of a d -quark generated by exchange of one Higgs boson and one W -boson, with a sizeable Higgs coupling $\sim g_W m_t/M_W$ to a top quark and where only *one* of the Higgs couplings are flavor changing. (In my notation, $g_W = g/\sqrt{2}$ is the W -boson coupling to fermions and g is the $SU(2)_L$ gauge coupling). The non-crossed version to the left in Fig. 3 does not give a non-suppressed contribution. Taking crossed Higgs and W -bosons are equivalent to the topologies in the middle and right of Fig. 3.

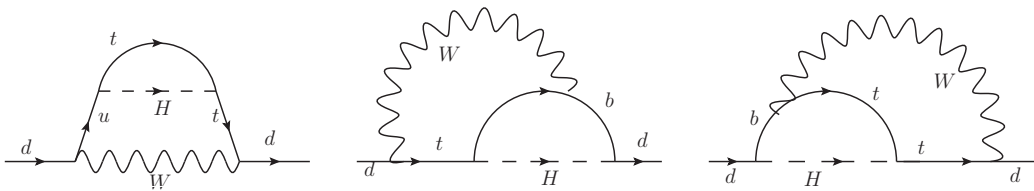


FIG. 3: Three diagrams with FC Higgs coupling for EDMs of a d -quark. Soft photon emission from one of the charged particles is assumed to be added. The left diagram will give contributions suppressed by $m_{u,d}/M_W$. Taking the crossed diagrams in the center or to the right, we will get contributions which are not suppressed by light quark masses. The diagram to the right is the complex conjugate of the diagram in the center.

Adding a soft photon to the diagram in the middle and to the right, we get four diagrams for both cases. In Fig. 4 the four diagrams obtained by adding a soft photon emission to the diagram to the right in Fig. 3 are shown. There are also similar diagrams for EDM of an u -quark. But in that case the ordinary SM coupling of the Higgs will be proportional to m_b/M_W instead of m_t/M_W for the d -quark case. We therefore expect that contributions to the u -quark EDM are suppressed for diagrams considered in this section. And in fact it turns out that u -quark contributions are suppressed by a factor of order $(m_b/m_t)^2 \sim 10^{-3}$ compared to the analogous d -quark contributions. Therefore the u -quark dipole moments due to diagrams in Fig.4 are neglected. For the same reason contributions to the d -quark dipole moment with the top replaced by the u - or c -quark are suppressed by $(m_u/m_t)^2$ and $(m_c/m_t)^2$, respectively, and are safely neglected in this section.

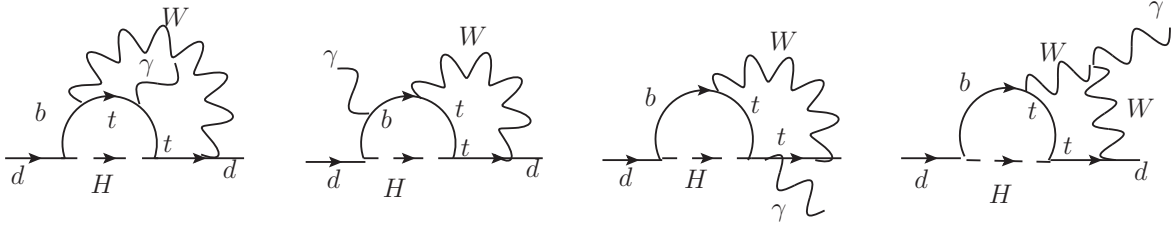


FIG. 4: Four diagrams for an EDM of a d quark obtained by adding a soft photon to the diagram to the right of Fig. 3. The left diagram is the same as in Fig. 1, with obvious particle replacements. For the first three diagrams, there are also corresponding diagrams where the W -boson is replaced by an unphysical Higgs-boson within Feynman gauge.

The various loop contributions to the EDM of a fermion $f(=u,d)$ from diagrams shown at the right of Fig. 3 (with a soft photon added, and like Fig. 4, and later in Fig. 6) have the form

$$\mathcal{M}(f \rightarrow f\gamma)_{(a)} = A (\bar{f} \sigma \cdot F P_R f) . \quad (12)$$

The diagrams obtained from the centre of in Fig. 3, can be then written

$$\mathcal{M}(f \rightarrow f\gamma)_{(c)} = A^* (\bar{d} \sigma \cdot F P_L d) . \quad (13)$$

Thus the electric dipole moment is equal to

$$(d_f)_{2-loop} = 2 \operatorname{Im}(A). \quad (14)$$

There is also a contribution to the magnetic moment (i.e the gyromagnetic quantity $(g-2)$) given by $2 \operatorname{Re}(A)$.

In calculating two loop diagrams in Fig. 4 we enter expressions of the type given in eq. (53) in the Appendix. We first use two Feynman parameters in the first sub-loop. The result depends also on the loop momentum of the second sub-loop. Then we integrate over the virtual loop momenta of the second sub-loop. Further, one of the Feynman parameters from the first loop can easily be integrated out, while the integral over the last Feynman parameter is done numerically.

The contributions from the diagrams in Fig. 4 and its complex conjugates can be written

$$\left(\frac{d_d}{e}\right)_i = \hat{e}_i F S_i \operatorname{Im}[Y_R(d \rightarrow b) V_{td}^* V_{tb}] \quad (15)$$

where the \hat{e}_i 's are the electric charges (in units e = the proton charge) of the photon-emitting particles, i.e. $\hat{e}_{1,3} = \hat{e}_t = +2/3$, $\hat{e}_2 = \hat{e}_b = -1/3$, and $\hat{e}_4 = \hat{e}_W = +1$. Here we have used the relation (9) and (14). The V 's are CKM matrix elements in the standard notation. The constant F sets the overall scale of the EDMs obtained from our two loop diagrams:

$$F = \frac{g_W^3}{M_W \sqrt{2}} \left(\frac{1}{16\pi^2}\right)^2 = \frac{2M_W^2}{v^3} \left(\frac{1}{16\pi^2}\right)^2 \simeq 6.94 \times 10^{-22} \text{ cm}, \quad (16)$$

where $v = 246 \text{ GeV}$ is the electroweak symmetry breaking scale, and where we have used the conversion relation $1/(200\text{MeV}) = 10^{-13} \text{ cm}$.

Using the Feynman gauge for the W -boson, we need to add interactions with the unphysical Higgs field ϕ . The interaction Lagrangian for ϕ for $t \leftrightarrow d$ transitions is

$$\mathcal{L}_{\phi td} = -\frac{g_W}{M_W} V_{td}^* \bar{d} \phi_- (m_d P_L - m_t P_R) t + h.c., \quad (17)$$

and similar for $t \leftrightarrow b$ transitions. The quantities S_i in (15) are dimensionless and given by integrals over one Feynman parameter. For the first two diagrams, the loop functions S_1 and S_2 are finite, and numerically, we find

$$S_1 = -2.55 \quad ; \quad S_2 = 2.50. \quad (18)$$

If the soft photon is emitted from the top quark after exchange of the Higgs boson, as in the third diagram from left in Fig. 4, or from soft photon emission from the W -boson in the

fourth diagram, the left sub-loop containing the Higgs boson is logarithmically divergent. The result of the divergent part of this sub-loop can within cut-off regularization be written

$$Log(r^2, x, y, masses)_\Lambda = \frac{i}{16\pi^2} \cdot 2 \int_0^1 dx \int_0^{(1-x)} dy \left(\ln(\Lambda^2/R) - \frac{3}{2} \right) , \quad (19)$$

where Λ is the cut-off, and x and y are Feynman parameters, and

$$R \equiv Q - x(1-x)r^2 ; \quad Q \equiv m_b^2 + x(M_W^2 - m_b^2) + y(M_H^2 - m_b^2) . \quad (20)$$

Here r^2 is the loop momentum squared for the other sub-loop. The left sub-loop also contains genuinely finite terms which can be written

$$Fin(r^2, x, y, masses) = \frac{i}{16\pi^2} \cdot 2 \int_0^1 dx \int_0^{(1-x)} dy \left(\frac{r^2 p(x)}{Q - (1-x)r^2} \right) , \quad (21)$$

where $p(x)$ is a second order polynomial in x .

The $\ln(\Lambda^2)$ term in (19) can easily be folded into the next subloop to obtain a simple expression, while the terms $\ln(R)$ in (19) and $Fin(r^2, x, y, masses)$ in (21) gives more complicated integrals. It turns out that for the third diagram the divergent part corresponding to (19) is projected out due to Dirac algebra (-technically, $\gamma_\alpha \sigma^{\mu\nu} \gamma^\alpha = 0$). We are then left with the finite part S_3^W corresponding to the function Fin above, and given in eq. (65) in the Appendix, as an integral over the function K in (66). However, adding the corresponding contribution with the W -boson replaced by the unphysical Higgs-boson, the divergence remains. As this divergences does not cancel with other divergent terms, it means that the theory based on the Lagrangian in eq. (7) alone is not renormalizable, meaning we are dealing with an effective theory. In the present case we have parametrized the logarithmic divergent part from exchange of the unphysical Higgs ϕ as

$$S_{3\Lambda}^\phi = \left(\frac{m_t^4}{M_W^2} \right) \cdot P(M_W^2; m_t^2) \cdot C_\Lambda = 3.42 C_\Lambda , \quad (22)$$

where

$$P(b, c) \equiv \frac{1}{c-b} \left(1 - \frac{b \ln(c/b)}{(c-b)} \right) ; \quad C_\Lambda \equiv \ln\left(\frac{\Lambda^2}{M_W^2}\right) + \frac{1}{2} . \quad (23)$$

Here C_Λ varies from ~ 5.5 to ~ 7.7 for $\Lambda \sim 1$ TeV to $\Lambda \sim 3$ TeV. Note that S_3^ϕ is of the order m_t^4 in contrast to $S_{1,2}$, S_3^W and S_4 which are of the order m_t^2 .

As usual a divergent logarithm is accompanied by a finite logarithm term $\ln(R)$ as seen in eqs (19), (59 and (60). This finite logarithmic term is given in the Appendix by an integral in

(68) over the function Z given in (69). The contributions corresponding to the function Fin is given as an integral in (70) over the function K in the Appendix in eq (66). Numerically, we obtain for the finite parts of the third diagram

$$S_3^W = 0.22 ; S_{3Z}^\phi = -1.90 , S_{3F}^\phi = 3.49 . \quad (24)$$

The fourth diagram in Fig. 4 with the soft photon emitted from the W -boson again contains a divergent part. Also in this case the divergent part does not go away, i.e. it is not cancelled against the previous divergent term. Then we find the logarithmic divergent term

$$S_{4\Lambda} = -\frac{3}{4}m_t^2 \cdot P(m_t^2; M_W^2) C_\Lambda = -0.91 C_\Lambda \quad (25)$$

The finite terms S_{4Z} and S_{4F} can also be written in terms of integrals over Z and K , as given in (71) and (72) in the Appendix. Numerically, we find for the finite parts of the fourth diagram,

$$S_{4Z} = 2.12 , S_{4F} = 0.86 . \quad (26)$$

Summing all contributions from diagrams in Fig. 4, we find

$$\left(\frac{d_d}{e}\right)_{Fig.4} = (1.65 + 1.37 C_\Lambda) \cdot F \cdot Im[Y_R(d \rightarrow b) V_{td}^* V_{tb}] \quad (27)$$

IV. DIAGRAMS WITH ONE FC COUPLING -AND A WWH -COUPLING

We will now consider another class of two loop diagrams generated by Higgs-boson FC couplings. These diagrams shown in Fig. 5 have a big WWH -coupling $\sim g_W M_W$ and only *one* FC Higgs coupling to a fermion.

These two loop diagrams are divided in three types: the (a)-diagrams with Higgs exchanges to the left, the (b)-diagrams with Higgs exchange in the middle, and the (c)-diagrams with Higgs exchange to the right. In the limit of zero external light quark momenta, which we work, the (b)-diagrams are zero due to (odd) momentum integration, or they are suppressed by small external quark masses. The (c)-diagrams are complex conjugates of the (a)-diagrams. Soft photon emission from one of the charged particles should of course be added in Fig. 5, as seen in Fig. 6 for the (a)-diagrams.

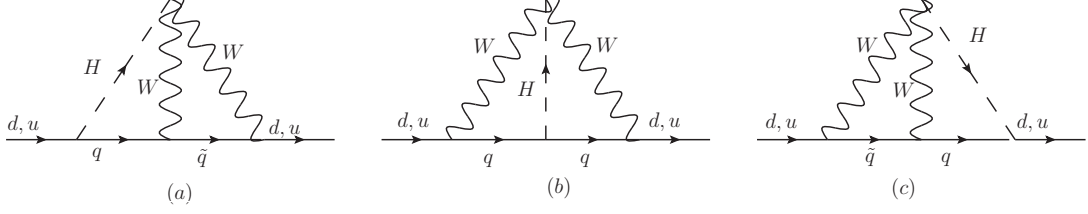


FIG. 5: The three diagrams of with FC Higgs coupling for EDMs of a u - or d -quark. Soft photon emission from one of the charged particles is assumed to be added. The (b) diagrams are zero in the limit of zero external momentum of the light quarks due to momentum integration. The (c) diagrams are complex conjugates of the (a) diagrams. Here $q = s, b$ and $\tilde{q} = u, c, t$ for EDM of a d -quark, and $q = c, t$ and $\tilde{q} = d, s, b$ for EDM of a u -quark.

The relevant piece of the SM Lagrangian for a Higgs coupling to two W -bosons is given by

$$\mathcal{L}_{\text{WWH}} = g_W M_W \sqrt{2} H W^{(-)\mu} W_\mu^{(+)} . \quad (28)$$

Using Feynman gauge for the W -boson, we must also consider Lagrangian terms involving an unphysical Higgs boson ϕ . Then the relevant $HW\phi$ - coupling is obtained from the Lagrangian

$$\mathcal{L}_{\text{HW}\phi} = \frac{g_W}{\sqrt{2}} \{ H (i\partial^\mu \phi_-) - (i\partial^\mu H) \phi_- \} W_\mu^{(+)} + h.c. \quad (29)$$

This means that the vertices involving the unphysical Higgs ϕ will depend on the loop momenta, which might give divergent (sub-)loops. There are also $W\phi\gamma$ -couplings, but they do not contribute for soft photon emission.

In the preceeding section all numerically relevant diagrams were proportional to m_t^2 , and even m_t^4 for S_3^ϕ . In this section the diagrams have another chiral structure, and we only get diagrams $\sim m_t^2$ for the case when the W -boson is replaced by an unphysical Higgs ϕ . Therefore we apriori consider all quark flavors in the loop, although it is expected that the GIM-mechanism might cancel the leading terms with one light quark flavor.

Contributions to the d -quark EDM from soft photon emission from the quark $q = s, b$ in the diagram (5a), i.e. to the left in Fig. 6 can be written :

$$\begin{aligned} \left(\frac{d_d}{e}\right)_q = & -2 \hat{e}_s F \{ \text{Im} [Y_R(d \rightarrow s) \lambda_u] \cdot \Delta f_d(s, u - c) + \text{Im} [Y_R(d \rightarrow s) \lambda_t] \cdot \Delta f_d(s, t - c) \} \\ & -2 \hat{e}_b F \{ \text{Im} [Y_R(d \rightarrow b) \xi_u] \cdot \Delta f_d(b, u - c) + \text{Im} [Y_R(d \rightarrow b) \xi_t] \cdot \Delta f_d(b, t - c) \} \quad (30) \end{aligned}$$

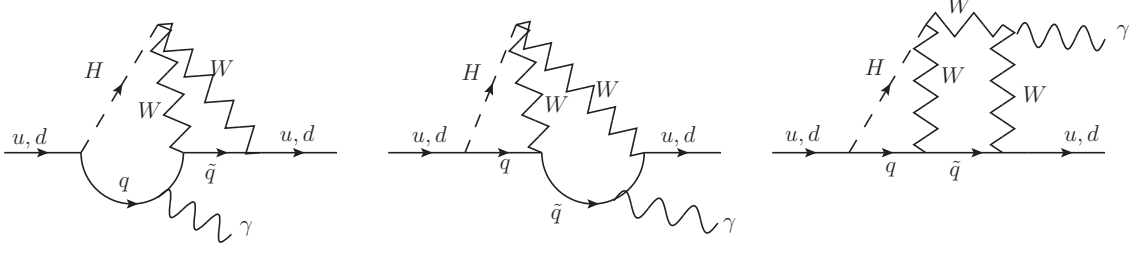


FIG. 6: Emission of a soft photon from (a)-type diagrams of Fig. 5. There is also a diagram with emission from the W in center of the diagram, and in addition additional graphs with the W replaced by an unphysical Higgs within Feynman gauge.

where F is given in (16) and where $\hat{e}_s = \hat{e}_b = -1/3$ are charges for the photon-emitting quarks, and the λ 's and the ξ 's are CKM factors:

$$\lambda_{\tilde{q}} = V_{\tilde{q}d}^* V_{\tilde{q}s} , \quad \xi_{\tilde{q}} = V_{\tilde{q}d}^* V_{\tilde{q}b} , \quad \tilde{q} = u, c, t , \quad (31)$$

Note that only the right-handed couplings Y_R contribute to the amplitude, due to the chiral structure of the two loop diagrams. Within the Wolfenstein parametrization, λ_t is of fifth order in $\lambda = \lambda_u$, while ξ_u and ξ_t are only of third order. Above , we have used the shortages

$$\Delta f_d(b, t - c) \equiv f(b, t) - f(b, c) \quad ; \quad \Delta f_u(t, b - s) \equiv f(t, b) - f(t, s) , \quad (32)$$

and so on in a self-explanatory way.

Similarly, contributions to the u -quark EDM due to emission from the quark $q = c, t$ the diagram to the left in Fig. 6 is :

$$\begin{aligned} \left(\frac{d_u}{e}\right)_q = & -2 \hat{e}_c F \{ \text{Im} [Y_R(u \rightarrow c) \kappa_d] \cdot \Delta f_u(c, d - s) + \text{Im} [Y_R(u \rightarrow c) \kappa_b] \cdot \Delta f_u(c, b - s) \} \\ & -2 \hat{e}_t F \{ \text{Im} [Y_R(u \rightarrow t) \zeta_d] \cdot \Delta f_u(t, d - s) + \text{Im} [Y_R(u \rightarrow t) \zeta_b] \cdot \Delta f_u(t, b - s) \} \end{aligned} \quad (33)$$

where the κ 's and the ζ 's are CKM factors:

$$\kappa_{\tilde{q}} = V_{u\tilde{q}} (V_{c\tilde{q}})^* , \quad \zeta_{\tilde{q}} = V_{u\tilde{q}} (V_{t\tilde{q}})^* , \quad \tilde{q} = d, s, b . \quad (34)$$

Within the Wolfenstein parametrization, $\kappa_d = -\lambda$, κ_b is of fifth order, while ζ_d and ζ_b are of third order in λ .

The quantities $f(q, \tilde{q})$ for given flavors q and \tilde{q} are functions of quark, W -boson and Higgs masses and involve logarithmic and dilogarithmic functions, and will be given below in the Appendix in terms of integrals over *one* Feynman parameter. In our previous paper [31] it was possible to extract leading logarithmic contributions because of a hierarchy of masses. In the present case this does not work because the masses of the Higgs boson H , the top quark t and the W -boson are of the same order of magnitude. The loop functions $f(q, \tilde{q})$ in eq. (30), (32), (33) are given by the explicit formulae in terms of the same function K in (66) as the finite parts of S_3 and S_4 in (65) and (72), but with other mass parameters. In the $f(q, \tilde{q})$'s the unphysical Higgs (ϕ) contributions within Feynman gauge for the W -boson are also included. The functions f are finite, and are of order 10^{-1} to 1. (See Table I and II). The GIM-cancellations for the difference between the u - and c -quark contributions are very efficient, making the differences $\Delta f_d(s, u - c)$ and $\Delta f_d(b, u - c)$ are of order 10^{-3} to 10^{-7} , and can be safely neglected. The differences between the c , and t -contributions are still of order 10^{-1} to 1. Numerically,

$$\Delta f_d(s, t - c) \simeq \Delta f_d(b, t - c) \simeq -0.34 \quad (35)$$

As the $f_d(q, u - c)$'s are very small, and λ_t is of order λ^5 , while ξ_t is of order λ^3 , we find that the contribution proportional to $\xi_t \cdot \Delta f_d(b, t - c)$ dominates in equation (30). Note that in this case it is necessary to know both the c - and the t -quark contributions to obtain $\Delta f_d(b, t - c)$. This is in contrast to the preceding section where the c -quark contributions could be neglected. For the EDMs of the u -quark, the values of the various (Δf_u) 's are of order 10^{-3} to 10^{-7} after GIM-cancellation, and can be neglected, as seen in table II in the Appendix.

Diagrams with soft photon emission from the quark $\tilde{q} = u, c, t$, are shown the center diagram in Fig. 6. Adding contributions where the W is replaced by an unphysical Higgs ϕ , we obtain divergent contributions for the loop functions $h(q, \tilde{q})$. Here the left subloop is divergent because the $WH\phi$ -vertex is momentum dependent. These divergences do not cancel among themselves, which again reflects the fact that the theory based on the Lagrangian in eq. (7) alone is not renormalizable, as also found in the preceding section. We have split the functions h in a logarithmic divergent part h_Λ , the associated finite logarithmic part h_Z coming from $\ln(R)$ in (19) due to unphysical Higgs, and the finite part h_F :

$$h = h_\Lambda + h_Z + h_F \quad (36)$$

The numerically relevant term is given by:

$$\left(\frac{d_d}{e}\right)_{\tilde{q}} = +2 \hat{e}_{\tilde{q}} F \cdot \text{Im} [\xi_t Y_R(d \rightarrow b)] \cdot \Delta h_d(b, t - c) , \quad (37)$$

where $\Delta h_d(b, t - c)$ is defined similar to the Δf 's in eq.(32). The full expression is given in eq. (78) in the Appendix. Also here the u -quark EDM d_u can be neglected (see eq. (79)).

Numerically, we find for the dominating quantities $\Delta h_d(b, t - c)$:

$$\Delta h_{d\Lambda} = m_t^2 \cdot P(m_t^2; M_W^2) \cdot C_\Lambda \simeq 1.22 C_\Lambda , \quad \Delta h_{dZ} = 0.39 , \quad \Delta h_{dF} = -1.65 , \quad (38)$$

For other cases the Δh 's are of order 10^{-3} or smaller. For the individual finite terms $h_F(q, \tilde{q})$ obtained before GIM-cancellations, some loop functions are also given by integrals (see (75)) over the function K in (66). Their numerical values are given in Tables III and IV. Similar to the case with emission from quark q , the contribution involving the top quark proportional to ξ_t gives the biggest contributions after GIM-cancellation, as in the preceeding section.

For diagrams with a soft photon emitted from the W -boson are shown in Fig. 6 we have used the effective W -propagator (52). Also in this case there are divergent diagrams, because the left sub-loop might be divergent for the replacement $W \rightarrow \phi$. Again we have split the functions k in a finite parts k_F , k_Z and a divergent part k_Λ due to unphysical Higgs:

$$k = k_\Lambda + k_Z + k_F . \quad (39)$$

Further details about the k -functions are given in the last part of the Appendix. After GIM-cancellation the dominant term is

$$\left(\frac{d_d}{e}\right)_W = 3 \hat{e}_W F \cdot \text{Im} [Y_R(d \rightarrow b) \xi_t] \cdot \Delta k_d(b, t - c) , \quad (40)$$

Numerically, we find for the parts of $\Delta k_d(b, t - c)$:

$$\Delta k_{d\Lambda} = \frac{1}{2} m_t^2 P(m_t^2; M_W^2) \cdot C_\Lambda \simeq 0.61 C_\Lambda ; \quad \Delta k_{dZ} = -0.38 , \quad \Delta k_{dF} = -2.10 , \quad (41)$$

Other Δk 's are of order 10^{-3} or smaller.

Neglecting small contributions (all except those proportional to $V_{td}^* V_{tb} \equiv \xi_t$), and summing all contributions from diagrams in Fig. 6 we find

$$\left(\frac{d_d}{e}\right)_{Fig.6} = (3.46 C_\Lambda - 9.35) \cdot F \cdot \text{Im}[Y_R(d \rightarrow b) V_{td}^* V_{tb}] \quad (42)$$

For the u -quark the EDM is suppressed by a factor of order 10^{-3} compared to the d -quark EDM.

V. SUMMARY AND DISCUSSION

As expected, there are cases where the considered two loop diagrams for the EDMs of d - and u -quarks diverges. This happens for cases in section III where the left sub-loop in Fig. 7 is involved, and for diagrams where the unphysical Higgs (ϕ) is involved both in sect III and IV. More specific, the left diagram in Fig. 7 which looks like a vertex correction for $d \rightarrow W + u, c, t$ is logarithmically divergent. And, actually, this diagram generates a logarithmic divergent *right-handed current* which has no match in the SM. We have parametrized the divergence in terms of C_Λ defined in (23), which is $\simeq 5.54$ for $\Lambda = 1$ TeV as used in [33], and $\simeq 7.74$ if $\Lambda = 3$ TeV

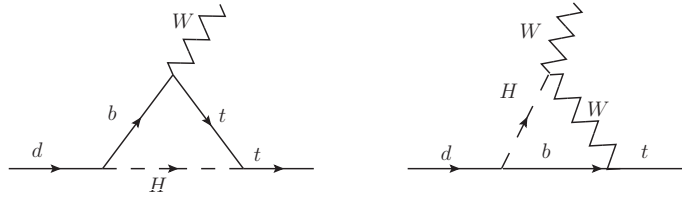


FIG. 7: The divergent effective W -loop vertex correction diagram relevant for diagrams of section III (left), and the (finite) effective vertex correction relevant for diagrams in section IV (right).

The right diagram in Fig. 7 is convergent, but if the W -boson is replaced by an unphysical Higgs ϕ when used in two loop diagrams, as in Fig. 6, we obtain logarithmic divergent diagrams, which are numerically relevant if the quark \tilde{q} is a top quark. The dominating divergent terms in section III and IV are proportional to m_t^2 (-or even m_t^4 in one case in section III). It should be noted that the first and last diagram in Fig. 6 are relevant for the EDM of the electron [41]. However, in this case the divergent terms would be proportional to powers of the tiny ν mass, instead of the t -quark mass.

Summing all contributions from section III and IV, we obtain the dominating contribution

$$\left(\frac{d_d}{e}\right)_{Tot} = (4.83 C_\Lambda - 7.70) F \text{Im}[Y_R(d \rightarrow b) V_{td}^* V_{tb}] \quad (43)$$

All contributions (after GIM-cancellation) not proportional to $\xi_t \equiv V_{td}^* V_{tb}$ can be neglected. There are bounds for some of the Y_R 's from [33, 34]. We note that because ξ_t is complex, there will be a EDM even if $Y_R(d \rightarrow b)$ is real!

Taking the loop functions at face value, and using the lattice values in (6) and absolute value of $V_{td}^* V_{tb}$ from [5] we obtain

$$d_n/e \simeq (0.82 \text{ to } 1.28) \times \text{Im} \left[Y_R(d \rightarrow b) \cdot \frac{V_{td}^* V_{tb}}{|V_{td}^* V_{tb}|} \right] \times 10^{-22} \text{ cm} . \quad (44)$$

In obtaining this result, we have neglected d_s for the following reason: The loop functions for the s -quark are numerically close to the ones for the d -quark. The CKM factor is bigger, but $\gamma_s/\gamma_d \simeq 10^{-2}$, such that the contribution to the result in (4) from the d_s is of order 5%. Also, because we are dealing with an effective theory with limited precision, we do not consider the mixing of color electric terms into the EDM term in (3) due to renormalization effects in perturbative QCD.

Using the bound in (1), the result (44) would correspond to

$$|\text{Im} \left[Y_R(d \rightarrow b) \cdot \frac{V_{td}^* V_{tb}}{|V_{td}^* V_{tb}|} \right]| \leq (2.0 \text{ to } 3.2) \times 10^{-4} . \quad (45)$$

to be compared with the slightly stricter, but same order of magnitude bound

$$|Y_R(d \rightarrow b)| \leq 1.5 \times 10^{-4} . \quad (46)$$

obtained from the bound on $|Y_R(d \rightarrow b)|^2$ given in [33, 34]. Thus, we have found a bound on the coupling $Y_R(d \rightarrow b)$ comparable to the previous bound, but not directly on the absolute value given as in [33, 34]. Turned around, if the bound on $Y_R(d \rightarrow b)$ found in [33, 34] is (almost) saturated, we have found that a nEDM just below the bound in (1) can not be excluded. In contrast, for the case $Y_R(d \rightarrow s)$, the term proportional to λ_t will be small because of the bound on $Y_R(d \rightarrow s)$ from $K - \bar{K}$ -mixing. Also the terms involving $Y_R(u \rightarrow c)$ will give small contributions due to bounds on from $D - \bar{D}$ -mixing.

The coupling $Y_R(u \rightarrow t)$ is not bounded from the analysis in [33, 34]. Using the values in tables II, IV and VI multiplying $Y_R(u \rightarrow t)$, we see that the contribution to nEDM from this coupling alone is

$$(d_n/e)_{(u \rightarrow t)} \simeq 3.7 \times \text{Im} \left[Y_R(u \rightarrow t) \cdot \frac{V_{ub} V_{tb}^*}{|V_{ub} V_{tb}^*|} \right] \times 10^{-27} \text{ cm} . \quad (47)$$

Using the bound in (1), this would correspond to the rather relaxed bound

$$|\text{Im} \left[Y_R(u \rightarrow t) \cdot \frac{V_{ub} V_{tb}^*}{|V_{ub} V_{tb}^*|} \right]| \leq 7.8 . \quad (48)$$

However, the decay $t \rightarrow H u$ is addressed in [35, 36], which finds a bound for absolute values of such couplings of order 3×10^{-2} .

It should be noted that within the SM there will also be effective interactions similar to the Lagrangians in (7) - (11) generated from Penguin-like one loop diagrams. These will typically give smaller coefficients than the bounds in [33, 34]. For instance for an on-shell b -quark we obtain an effective coupling

$$Y(b \leftrightarrow d)_{SM}^{OS} = \frac{g_W^3 m_b}{16\pi^2 M_W} V_{td}^* V_{tb} J_{bd} \quad (49)$$

where J_{bd} is a loop function of order 10^{-1} , making $Y(b \leftrightarrow d)_{SM}$ smaller than the bound for $Y_R(d \rightarrow b)$ in (45) and in [33, 34]. However, within a SM calculation, the $Y_R(d \rightarrow b)$ coupling must be replaced by the correct off-shell momentum dependent loop result, and the chiral structure of the SM generated $d \rightarrow b$ loop gives a three loop diagram result different and tiny compared to our two-loop result.

Also in case of the $Y_R(u \rightarrow t)$ interaction, one could compare with the SM generated decay $t \rightarrow H u$ with effective coupling

$$Y(t \rightarrow H u)_{SM} = \frac{g_W^3 m_b^2}{16\pi^2 M_W m_t} V_{tb}^* V_{ub} J_{ut} \quad (50)$$

where J_{ut} is some loop function depending on masses and being of order 10^{-1} . This contribution is of course several orders of magnitude below the very relaxed bound in (48). But also here the (three) loop (chiral and momentum dependence) effective off-shell structure will give tiny contributions if replaced by our $Y_R(u \rightarrow t)$.

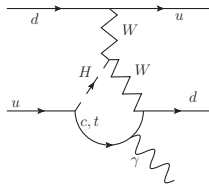


FIG. 8: Diagram with FC Higgs coupling for a diquark mechanism. A soft photon should be added.

Finally, it should be noted that also in this theory there are diquark contributions, as shown in Fig. 8, which we have not elaborated further because they are suppressed by uncertain hadronic effects.

VI. CONCLUSIONS

In the present paper the analysis in [33, 34] is extended to two loop case for quarks and EDMs generated by a flavor changing Higgs coupling Y_R to first order are considered. It is found that some contributions contain a certain divergent sub-loops for $d \rightarrow tW$ generated by the flavor changing Higgs. This divergent sub-loop corresponds to a generated right-handed current and will not contribute to renormalization of the left-handed current. This means that our theory based on (7) - (11) is only an effective one.

A complete theory renormalizable theory beyond the SM should be further built to be $SU(2)_L \times U(1)_Y$ symmetric and probably contain additional couplings and additional higher mass states. We have found two loop contributions which will give a bound for the imaginary part of $Y_R(d \rightarrow b)$ of the same order of magnitude as the authors of [33, 34] found for the absolute value from $B - \bar{B}$ -mixing. Turned around, if the bound for $Y_R(d \rightarrow b)$ found in [33, 34] is (almost) saturated, a value for nEDM just below the bound in (1) cannot be excluded. However, having only an effective theory depending on a cut-off, precise predictions cannot be given.

VII. APPENDIX

To simplify calculations we use the effective quark propagator in a soft electromagnetic field F [42]

$$S_1(k, F) = \left(-\frac{e_q}{4}\right) \frac{\{(\gamma \cdot k + m_q), \sigma \cdot F\}}{(k^2 - m_q^2)^2}, \quad (51)$$

where k is the four momentum and m_q the mass of the quark q . We use the notation $\{A, B\} \equiv AB + BA$. Similarly, for emission from a W -boson:

$$(D_1(k, F))^{\alpha\beta} = \left(-\frac{e_W}{4}\right) \frac{3i \{g^{\mu\alpha} g^{\nu\beta} - g^{\mu\beta} g^{\nu\alpha}\} F_{\mu\nu}}{(k^2 - M_W^2)^2}. \quad (52)$$

As an example we write down the loop integral for the diagram with soft photon emission from a t -quark, like the diagram in the middle of Fig. 6 (for $q = b$ and $\tilde{q} = t$):

$$T_{\mu\nu} = \int \int \frac{\bar{d}p \bar{d}r p_\mu r_\nu}{(p^2 - M_H^2)(p^2 - m_b^2)((r - p)^2 - M_W^2)(r^2 - M_W^2)(r^2 - m_t^2)^2}. \quad (53)$$

where $\bar{d}r \equiv d^d r / (2\pi)^d$ in d dimensions within dimensional regularization. An ultraviolet divergence appears if there is an additional $p_\mu p_\nu$ term in the numerator when doing loop

integration in the subloop containing the integration over p . This can happen when the W -is replaced by an unphysical Higgs within Feynman gauge, or if the left diagram in Fig. 7 is involved. Many loop diagrams are suppressed because of chirality ($P_L P_R = 0$), or asymmetric momentum integration:

$$\int \bar{d}p f(p^2; \text{masses}) p^\mu = 0 . \quad (54)$$

The quantities S_i in (15) are dimensionless and given by integrals over one Feynman parameter. For the first diagram in Fig. 4 we find

$$S_1 = -u \int_0^1 \frac{dx [(1-3x) - \frac{u}{2}(1-x)]}{(u-1)(1-x)} \left\{ \ln \frac{C_1}{C_0} - \frac{H}{C_1-H} \ln\left(\frac{C_1}{H}\right) + \frac{H}{C_0-H} \ln\left(\frac{C_0}{H}\right) \right\} . \quad (55)$$

We have introduced the mass ratios $u \equiv \frac{m_t^2}{M_W^2}$ and $H \equiv \frac{M_H^2}{M_W^2}$, where M_H is the Higgs mass. Terms suppressed by a factor of order m_b^2/m_t^2 with respect to the terms in (55) are neglected. Further, we have

$$C_0 \equiv C_0(x) = \frac{u}{x(1-x)} , \quad C_1 \equiv C_1(x) = \frac{1+x(u-1)}{x(1-x)} . \quad (56)$$

The term $\frac{u}{2}(1-x)$ in the numerator in (55) is due to the unphysical Higgs contribution which have to be added when we use Feynman gauge for the W -propagator.

If the soft photon is emitted from the b -quark in the second diagram from left in Fig. 4 we obtain

$$S_2 = -\frac{u(1+\frac{u}{2})}{2(u-1)} \int_0^1 dx (1-2x) \left\{ -\text{dilog}\left(\frac{C_1}{H}\right) + \text{dilog}\left(\frac{C_0}{H}\right) \right\} , \quad (57)$$

where C_0 and C_1 are given as in (56) and the term proportional to $u \cdot u/2$ in the numerator is the unphysical Higgs contribution. The dilogarithmic function is in our case defined as

$$\text{dilog}(z) = \int_1^z dt \frac{\ln(t)}{(1-t)} = \text{Li}_2(1-z) , \quad (58)$$

If the soft photon is emitted from the top quark after exchange of the Higgs boson, as in the third diagram from left in Fig. 4, or from soft photon emission from the W -boson in the fourth diagram, the left sub-loop containing the Higgs boson is logarithmically divergent. The result of the divergent part of this sub-loop, written as in (19), can further be rewritten as

$$\text{Log}(r^2, x, y, \text{masses})_\Lambda = \frac{i}{16\pi^2} \left[C_\Lambda - 2 \int_0^1 dx \int_0^{(1-x)} dy L_Z(r^2, x, y, \text{masses}) \right] , \quad (59)$$

where C_Λ is given in (23) and where we have pulled out the factor $x(1-x)$ from the logarithm $\ln(R) = \ln[-x(1-x)r^2 + Q]$ in (59), and using $\int_0^1 dx x \ln(x(1-x)) = -1$, we obtain

$$L_Z(r^2, x, y, masses) = \ln \left[-r^2 + \frac{Q}{x(1-x)} \right] - \ln(M_W^2) . \quad (60)$$

These loop expressions should then be folded into the loop integral

$$J = \int \frac{\vec{d}r}{(r^2 - M_W^2)(r^2 - m_t^2)^2} \cdot Func(r^2, x, y, masses) , \quad (61)$$

where $Func$ is Log or Fin above. We can now perform the loop integration over virtual euclidian squared momentum $\eta = -r^2$, using

$$\vec{d}r \rightarrow \frac{i}{16\pi^2} \eta d\eta \quad (62)$$

For $Func = const$, i.e. independent of r^2, x, y , we find

$$J = \frac{-i}{16\pi^2} P(M_W^2; m_t^2) \cdot const \quad (63)$$

where $P(b, c)$ is given in (23). The eqs. (61) and (63) are relevant for the logarithmic divergent term because C_Λ is independent of the Feynman parameters of the first subloop and the loop momentum r of the second sub-loop.

The y -integration in (59) and (21) can be done by using

$$dy = \frac{x(1-x)}{M_H^2 - m_b^2} \cdot d\tilde{Q} \quad ; \quad \tilde{Q} \equiv \frac{Q}{x(1-x)} , \quad (64)$$

and we obtain the integrals over the last Feynman parameter x in (65) - (72) in the Appendix.

For the third diagram in Fig. 4 we find for the remaining finite part in S_3 after the Dirac-algebra has killed the divergent part in this case:

$$S_3^W = \frac{u}{2(H-b)} \int_0^1 dx x (K(1, u; B_1) - K(1, u; B_0)) \quad (65)$$

where the functions K are in general given by

$$\begin{aligned} K(A, a; B) &\equiv -\frac{a}{(A-a)} \ln(B) + \frac{a^2}{(A-a)(B-a)} \ln\left(\frac{B}{a}\right) \\ &- \left(\frac{A}{A-a}\right)^2 \text{dilog}\left(\frac{B}{A}\right) + \left[\left(\frac{A}{A-a}\right)^2 - 1\right] \text{dilog}\left(\frac{B}{a}\right) \end{aligned} \quad (66)$$

where in (65)

$$B_0 \equiv \frac{\tilde{Q}(y=0)}{M_W^2} = \frac{b+x(u-b)}{x(1-x)} ; \quad B_1 \equiv \frac{\tilde{Q}(y=1-x)}{M_W^2} = \frac{H+x(u-H)}{x(1-x)} . \quad (67)$$

where $b \equiv \frac{m_b^2}{M_W^2}$, $u \equiv \frac{m_t^2}{M_W^2}$, and $H \equiv \frac{M_H^2}{M_W^2}$.

For the third diagram in Fig. 4, with W replaced by the unphysical Higgs ϕ the contribution corresponding to L_Z in (59) is

$$S_{3Z}^\phi = -\frac{u^2}{(H-b)} \int_0^1 dx x(1-x)[Z(1, u; B_1) - Z(1, u; B_0)] \quad (68)$$

where in general:

$$\begin{aligned} Z(C, A; B) \equiv & \frac{(A^2 - AB)}{C - A} \left(\frac{\ln(B)}{A} + \frac{\ln(\frac{B}{A})}{(B - A)} \right) \\ & + \frac{C(C - B)}{(C - A)^2} \left\{ \frac{1}{2} [\ln(B - C)]^2 + \text{dilog}\left(\frac{B}{B - C}\right) - \ln(C) \cdot \ln(B - C) \right\} \\ & + \frac{[BC - A(2C - A)]}{(C - A)^2} \left\{ \frac{1}{2} [\ln(B - A)]^2 + \text{dilog}\left(\frac{B}{B - A}\right) - \ln(A) \cdot \ln(B - A) \right\}. \end{aligned} \quad (69)$$

Further for the corresponding finite part:

$$S_{3F}^\phi = \frac{u^2}{2(H-b)} \int_0^1 dx x(2x-3) (K(1, u; B_1) - K(1, u; B_0)) , \quad (70)$$

For the fourth (divergent) diagram with soft photon emission from the W -boson, we find

$$S_{4Z} = \frac{3u}{2(H-b)} \int_0^1 dx x(1-x)[Z(u, 1; B_1) - Z(u, 1; B_0)] \quad (71)$$

and for the corresponding finite term

$$S_{4F} = -\frac{3u}{2(H-b)} \int_0^1 dx x(x-2) (K(u, 1; B_1) - K(u, 1; B_0)) . \quad (72)$$

and where $B_{1,0}$ are given as in (67).

The mathematical expression for the loop functions $f(q, \tilde{q})$ for soft photon emission from the quark q given in the left of Figure 6 is given as

$$f(q, \tilde{q}) = \frac{1}{1-b} \int_0^1 dx [K(H, a; D_1) - K(H, a; D_0)] \left\{ x - \frac{b}{4} (1-2x) \right\} , \quad (73)$$

where $a \equiv \frac{(m_q)^2}{M_W^2}$, $b \equiv \frac{(m_{\tilde{q}})^2}{M_W^2}$, and $H \equiv \frac{M_H^2}{M_W^2}$

$$D_0 \equiv D_0(x) \equiv \frac{b+x(1-b)}{x(1-x)} \quad D_1 \equiv D_1(x) \equiv \frac{1}{x(1-x)} . \quad (74)$$

The f -functions are not directly proportional to quark masses as for the S_i functions in section III. Therefore the individual terms are calculated separately before performing the

GIM-cancellation, namely, to obtain $f(b, t - c)$, both $f(b, t)$ and $f(b, c)$ are needed. The same is the case for $h(b, t - c)$ and $k(b, t - c)$ below. This is in contrast to the amplitudes in section III, where diagrams involving to c -quark can be safely neglected.

The numbers for the f 's are given in tables I and II below.

quark \tilde{q}	$f(s, \tilde{q})$	$f(b, \tilde{q})$
u	0.296731	0.293166
c	0.296656	0.293092
t	-0.047004	-0.047305

TABLE I: Values for the loop function $f(q, \tilde{q})$ for EDM of the d quark, see eqs. (27-29)

quark \tilde{q}	$f(c, \tilde{q})$	$f(t, \tilde{q})$
d	0.2962815	1.136204
s	0.2962810	1.136201
b	0.2954856	1.131829

TABLE II: Values for the loop functions $f(q, \tilde{q})$ for EDM of the u quark; see eqs. (27-29)

For emission from the quark \tilde{q} similar to (73), but with M_H replaced by M_W and $m_q \leftrightarrow m_{\tilde{q}}$ i.e $H \rightarrow 1$ and $a \leftrightarrow b$. Here h_F is the finite part given by

$$h_F(q, \tilde{q}) = \frac{1}{H - a} \int_0^1 dx x (1 - \frac{b}{2}(1 + x)) [K(1, b; B_1) - K(1, b; B_0)] \quad (75)$$

where a, b, H are given as below (73).

$$B_1 = \frac{H + x(1 - H)}{x(1 - x)}; \quad B_0 = \frac{a + x(1 - a)}{x(1 - x)}. \quad (76)$$

The term proportional to $b/2$ above is the finite part of the unphysical Higgs contribution. The functions h_F are given in tables III and IV.

The term $h_Z(q, \tilde{q})$ is given by

$$h_Z(q, \tilde{q}) = -\frac{b}{(H - a)} \int_0^1 dx x (1 - x) (Z(1, b; B_1) - Z(1, b; B_0)) , \quad (77)$$

where $B_{0,1}$ are given as in (76).

quark \tilde{q}	$h_F(s, \tilde{q})$	$h_F(b, \tilde{q})$
u	0.348206	0.347882
c	0.347396	0.347073
t	-1.300107	-1.298341

TABLE III: Values for the loop function h_F for EDM of the d quark

quark \tilde{q}	$h_F(c, \tilde{q})$	$h_F(t, \tilde{q})$
d	0.3481758	0.2108653
s	0.3481687	0.2108620
b	0.3417355	0.2077501

TABLE IV: Values for the loop function h_F for EDM of the u quark

The full expressions for contributions from soft photon emission from the quark $\tilde{q} = u, c, t$, i.e the center diagram in Fig. 6, is given by:

$$\begin{aligned} \left(\frac{d_d}{e}\right)_{\tilde{q}} = & +2 \hat{e}_{\tilde{q}} F \{ \text{Im} [Y_R(d \rightarrow s) \lambda_u] \cdot \Delta h_d(s, u - c) + \text{Im} [Y_R(d \rightarrow s) \lambda_t] \cdot \Delta h_d(s, t - c) \} \\ & + 2 \hat{e}_{\tilde{q}} F \{ \text{Im} [Y_R(d \rightarrow b) \xi_u] \cdot \Delta h_d(b, u - c) + \text{Im} [Y_R(d \rightarrow b) \xi_t] \cdot \Delta h_d(b, t - c) \} \end{aligned} \quad (78)$$

And for the u -quark with $\tilde{q} = d, s, b$

$$\begin{aligned} \left(\frac{d_u}{e}\right)_{\tilde{q}} = & +2 \hat{e}_{\tilde{q}} F \{ \text{Im} [Y_R(u \rightarrow c) \kappa_d] \cdot \Delta h_u(c, d - s) + \text{Im} [Y_R(u \rightarrow c) \kappa_b] \cdot \Delta h_u(c, b - s) \} \\ & + 2 \hat{e}_{\tilde{q}} F \{ \text{Im} [Y_R(u \rightarrow t) \zeta_d] \cdot \Delta h_u(t, d - s) + \text{Im} [Y_R(u \rightarrow t) \zeta_b] \cdot \Delta h_u(t, b - s) \} \end{aligned} \quad (79)$$

where $\hat{e}_{\tilde{q}} = \hat{e}_c = \hat{e}_t = 2/3$ are charges for the photon-emitting quarks $\tilde{q} = d, s, b$.

Now, the next step is to calculate the loop diagrams when the soft photon is emitted from a W -boson. For the diagram to the right in Fig. 6 the result is

$$k(q, \tilde{q})_1 = \frac{1}{(H - a)} \int_0^1 dx x [K(b, 1; B_1) - K(b, 1; B_0)] . \quad (80)$$

where $B_{0,1}$ are given as in (76).

When the soft photon is emitted from the W -boson in the middle of diagram we obtain

$$k(q, \tilde{q})_2 = \frac{1}{(H - a)} \int_0^1 \frac{dx x}{1 - x} [K_{W2}(B_1) - K_{W2}(B_0)] , \quad (81)$$

where the function $K_{W2}(B)$ is given by

$$K_{W2}(B) = \frac{B^2 \ln(B)}{(B - 1)(B - b)} . \quad (82)$$

with $B_{0,1}$ still given as in (76).

When the W in the middle is replaced by an unphysical Higgs, we obtain

$$k_3 = (k_\Lambda + k_Z) + \frac{b}{4} k_1 + \tilde{k}_3, \quad (83)$$

where

$$k_Z(q, \tilde{q}) = -\frac{b}{2(H-a)} \int_0^1 dx x(1-x) (Z(1, b; B_1) - Z(1, b; B_0)) , \quad (84)$$

and

$$\tilde{k}(q, \tilde{q})_3 = \frac{-b}{4(H-a)} \int_0^1 dx x^2 [K(b, 1; B_1) - K(b, 1; B_0)] , \quad (85)$$

where $B_{0,1}$ are given as in (76).

When the W to the right is replaced by an unphysical Higgs we obtain

$$k(q, \tilde{q})_4 = -\frac{b}{4} k(q, \tilde{q})_2 + \tilde{k}(q, \tilde{q})_4 , \quad (86)$$

with

$$\tilde{k}(q, \tilde{q})_4 = \frac{-b}{4(H-a)} \int_0^1 dx x [K_{W4}(B_1) - K_{W4}(B_0)] , \quad (87)$$

where

$$K_{W4}(B) = \Delta K_{W4}(B) + \frac{x}{(1-x)} K_{W2}(B) , \quad (88)$$

where $K_{W2}(B)$ is given previously in eq (82), and where

$$\Delta K_{W4}(B) = \frac{2}{(1-b)} \left(b \cdot \text{dilog}\left(\frac{B}{b}\right) - \text{dilog}(B) \right) , \quad (89)$$

The total finite amplitude is

$$k_F = k_1(1 + b/4) + k_2(1 - b/4) + \tilde{k}_3 + \tilde{k}_4 , \quad (90)$$

and the numerical values for the amplitudes k_F are given in tables V and VI. In eqs. (80) and (81) the terms proportional to $b/4$ are due to the unphysical Higgs contribution in Feynman gauge.

For diagrams with a soft photon emitted from the W -boson in Fig. 6 we have used the effective W -propagator (52) and the full expressions are

$$\begin{aligned} \left(\frac{d_d}{e}\right)_W = & 3 \hat{e}_W F \{ \text{Im} [Y_R(d \rightarrow s) \lambda_u] \cdot \Delta k_d(s, u - c) + \text{Im} [Y_R(d \rightarrow s) \lambda_t] \cdot \Delta k_d(s, t - c) \} \\ & + 3 \hat{e}_W F \{ \text{Im} [Y_R(d \rightarrow b) \xi_u] \cdot \Delta k_d(b, u - c) + \text{Im} [Y_R(d \rightarrow b) \xi_t] \cdot \Delta k_d(b, t - c) \} \end{aligned} \quad (91)$$

quark \tilde{q}	$k(s, \tilde{q})_F$	$k(b, \tilde{q})_F$
u	0.862602	0.862201
c	0.861867	0.861466
t	-1.229824	-1.234307

TABLE V: Values for the loop function k_F for EDM of the d quark

quark \tilde{q}	$k(c, \tilde{q})_F$	$k(t, \tilde{q})_F$
d	0.862565	0.585069
s	0.862561	0.585067
b	0.858181	0.582868

TABLE VI: Values for the loop function k_F for EDM of the u quark

and similarly, for EDM of the u -quark:

$$\begin{aligned} \left(\frac{d_u}{e}\right)_W = & 3 \hat{e}_W F \left\{ \text{Im} [Y_R(u \rightarrow c) \kappa_d] \cdot \Delta k_u(c, d - s) + \text{Im} [Y_R(u \rightarrow c) \kappa_b] \cdot \Delta k_u(c, b - s) \right\} , \\ & + 3 \hat{e}_W F \left\{ \text{Im} [Y_R(u \rightarrow t) \zeta_d] \cdot \Delta k_u(t, d - s) + \text{Im} [Y_R(u \rightarrow t) \zeta_b] \cdot \Delta k_u(t, b - s) \right\} \end{aligned} \quad (92)$$

where the κ 's and the ζ 's are CKM factors and $\hat{e}_W = +1$ is the W - charge, and the factor 3 is just the prefactor in the effective W -propagator in (52). Also in this case there are divergent diagrams, because the left sub-loop might be logarithmically divergent when the W -boson is replaced by the unphysical Higgs ϕ .

Acknowledgments

I am grateful to Svjetlana Fajfer for suggesting these calculations and for valuable discussions. Useful comments by Lluís Oliver and Ivica Picek are also acknowledged.

I am supported in part by the Norwegian research council (via the HEPP project).

-
- [1] M. Pospelov and A. Ritz, *Annals Phys.* **318** (2005) 119 [hep-ph/0504231]
 - [2] T. Fukuyama, *Int. J. Mod. Phys.* **A27** (2012) 1230015, arXiv: 1201.4252 [hep-ph]
 - [3] W. Dekens, J. de Vries, J. Baisou, W. Bernreuther, C. Hanhart, Ulf-G. Meiner, A. Nogga, and A. Wirzba *JHEP* **07** (2014) 069, arXiv:1404.6082[hep-ph]

- [4] M. Jung and A. Pich, JHEP **1404** 076, arXiv:1308.6283 [hep-ph]
- [5] K. A. Olive et al [Particle Data Group Collaboration] : “*Review of Particle Physics*”, *Chin. Phys.* **C40** (2016) 100001
- [6] C. A. Baker, D. D. Doyle, P. Geltenbort, K. Green, M. G. D. van der Grinten, P. G. Harris, P. Iaydjiev and S. N. Ivanov *et al.*, Phys. Rev. Lett. **97** (2006) 131801 [hep-ex/0602020].
- [7] A. Maiezza, and M. Nemevšek, *Phys. Rev.* **D 90** (2014) 095002, arXiv:1407.3678 [hep-ph]
- [8] E.P. Shabalin, E.P., *Yad.Fiz.* **31** (1980)1665-1679 (*Sov. J. Nucl.Phys.* **31** (1980) 864)
- [9] A. Czarnecki, and B. Krause, *Phys.Rev.Lett.* **78** (1997) 4339 [hep-ph/97043559]
- [10] D.V. Nanopoulos, A. Yildiz, and P. H. Cox, *Phys.Lett.* **B87** 53
- [11] B.F. Morel, *Nucl.Phys.* **B157** (1979) 23
- [12] M.B. Gavela, A. Le Yaouanc, L. Oliver,O. Pene J.C. Raynal, and T.N. Pham, *Phys.Lett.* **B109** (1982) 215
- [13] I.B. Khriplovich and A.R. Zhitnitsky, *Phys.Lett.* **B109** (1982) 490
- [14] B.H.J. McKellar,S.R. Choudhury, X.-G. He and S. Pakvasa, Phys.Lett. **B197** (1987) 556
- [15] J.O. Eeg, J.O. and I. Picek, *Phys.Lett.* **B130** (1983) 308
- [16] J.O. Eeg, and I. Picek, *Nucl.Phys.* **B244** (1984) 77
- [17] C. Hamzaoui and A. Barroso, Phys. Lett. B **154**, 202 (1985).
- [18] T. Mannel and N. Uraltsev, Phys. Rev. D **85** (2012) 096002, arXiv:1202.6270 [hep-ph]
- [19] T. Bhattacharya, V. Cirigliano, R. Gupta, H-W. Lin, and B. Yoon, *Phys. Rev. Lett.* **115** (2015) 212002, arXiv:1506.04196 [hep-lat]
- [20] T. Bhattacharya, V. Cirigliano, S. D. Cohen, R. Gupta, A. Joseph, H-W. Lin, and B. Yoon, *Phys. Rev.* **D 92** (2015)094511 , arXiv:1506.06411 [hep-lat]
- [21] W. Buchmuller and D. Wyler, *Phys.Lett.* **B121** (1983) 321
- [22] W. Altmannshofer, A. J. Buras and P. Paradisi, Phys. Lett. B **688** (2010) 202 [arXiv:1001.3835 [hep-ph]].
- [23] A. J. Buras, G. Isidori and P. Paradisi, Phys. Lett. B **694** (2011) 402, arXiv:1007.5291 [hep-ph]
- [24] J. Brod, U. Haisch, and J. Zupan, JHEP **1311** (2013) 180, arXiv:1310.1385 [hep-ph]
- [25] A. V. Manohar and M. B. Wise, Phys. Rev. D **74** (2006) 035009 [hep-ph/0606172].
- [26] G. Degrandi and P. Slavich, Phys. Rev. D **81** (2010) 075001, arXiv:1002.1071 [hep-ph]
- [27] Xiao-Gang He, Chao-Jung Lee, Siao-Fong Li, and J. Tandean, arXiv:1404.4436 [hep-ph]
- [28] J. M. Arnold, B. Fornal and M. B. Wise, Phys. Rev. D **87** (2013) 075004, arXiv:1212.4556

[hep-ph]

- [29] K. Fuyuto, J. Hisano, and E. Senaha, arXiv:1510.04485 [hep-ph]
- [30] W. Altmannshofer, R. Primulando, C. -T. Yu and F. Yu, *JHEP* **1204** (2012) 049, arXiv:1202.2866 [hep-ph]
- [31] S. Fajfer, and J.O. Eeg, *Phys. Rev.* **D89** (2014) 095030, arXiv:1401.2275 [hep-ph]
- [32] A. Goudelis, O. Lebedev, and J-h. Park, *Phys. Lett.* **B707** (2012) 369-374, arXiv:1111.1715 [hep-ph]
- [33] G. Blankenburg, J. Ellis, and G. Isidori, *Phys. Lett.* **B712** (2012) 386-390; arXiv:1202.5704 [hep-ph]
- [34] R. Harnik, J. Kopp and J. Zupan *JHEP* **03** (2013) 036, arXiv:1209.1397 [hep-ph]
- [35] A. Greljo, and J.F. Kamenik, and J. Kopp, *JHEP* **07** (2014) 046 arXiv 1404.1278 [hep-ph]
- [36] M. Gorbahn, and U. Haisch, *JHEP* **06** (2014) 033, arXiv 1404.4873 [hep-ph]
- [37] S.M. Barr and A. Zee, *Phys. Rev. Lett.* **65** (1990) 21-24 [Erratum: *Phys. Rev. Lett.* **65** (1990) 2920]
- [38] D.Chang, W.S. Hou, and W.-Y. Keung,, *Phys. Rev.***D48** (1993) 217; hep-ph/9302267
- [39] R.G. Leigh, R. G., S. Paban, S. and R. M. Xu, *Nucl. Phys.* **B352** (1991) 45-58
- [40] J.D. Bjorken, and S. Weinberg, *Phys. Rev. Lett.* **38** (1977) 622
- [41] W. Altmannshofer, J. Brod, and M. Schmaltz, *JHEP* **05** (2015) 125, arXiv 1503.04830 [hep-ph]
- [42] L.J Reinders, H. Rubinstein, and S. Yazaki, *Phys.Rept.* **127** (1985) 1